

First experimental evidence of de-twinning during reverse loading of TWIP steel

Scott J. McCormack¹, Azdiar A. Gazder², Elena V. Pereloma^{1,2}, Ahmed A. Saleh^{1*}

¹ School of Mechanical, Materials, Mechatronic and Biomedical Engineering, University of Wollongong, New South Wales 2522, Australia

² Electron Microscopy Centre, University of Wollongong, New South Wales 2500, Australia

Abstract: The present work investigates the effect of reverse (tension-compression) loading on the microstructure evolution in a fully annealed Fe-24Mn-3Al-2Si-1Ni-0.06C (wt.%) TWinning-induced plasticity (TWIP) steel. Electron back-scattering diffraction (EBSD) maps were acquired on the same selected area at true strains of 0% (initial), 12.8% (after forward tension loading) and 3.1% (after reverse compression loading). After forward tension loading to 12.8% true strain, deformation twins were observed to evolve preferentially in grains with orientations close to $\langle 111 \rangle$ and $\langle 110 \rangle$ parallel to the tensile axis. Subsequent reverse compression loading back to a true strain of 3.1% led to the removal of all deformation twins, providing the first unambiguous experimental evidence of de-twinning during load reversal in TWIP steel, in particular, and low SFE polycrystalline fcc materials, in general. This de-twinning process upon load reversal can be ascribed to the possibility of the reverse glide of the partial dislocations bounding the deformation twin, which in turn leads to the reorientation of the twin to match the parent grain.

1. INTRODUCTION

TWinning Induced Plasticity (TWIP) steels containing 20-30 wt.% Mn and small additions of Al and Si are a grade of advanced high strength steels suitable for automotive applications due to their unique combination of high strengths (600-1000 MPa) and large ductilities (>50%) [1]. TWIP steels possess a stable face centred cubic (fcc) austenite phase with low stacking fault energy (SFE = 18-40 mJ m⁻²) that instigate twinning along with dislocation glide during room temperature deformation. This low SFE also facilitates the dissociation of perfect dislocations gliding on the $\{111\}$ plane in the $\langle 110 \rangle$ direction into $\langle 112 \rangle$ Shockley partials bounding stacking faults.

While tracking the microstructure evolution during monotonic loading of TWIP steel has been the focus of numerous studies (see [2, 3] and the references therein), the characterisation of its cyclic (reverse) loading behaviour remains very limited. In this regard, a Fe-24Mn-3Al-2Si-1Ni-0.06C TWIP steel subjected to $\pm 1\%$ cyclic (tension-compression) loading was recently investigated using a combination of in-situ neutron diffraction and a modified elasto-plastic self-consistent modelling scheme [4, 5]. The modelling work in Ref. [4] raised the possibility that de-twinning events associated with the reversibility of slip along the $\langle 112 \rangle$ direction could be occurring upon load reversal. However, to the best of our knowledge, no unambiguous experimental observation of de-twinning has been made, to date, in coarse-grained (micron-sized) polycrystalline fcc materials.

To this end, the present study uses the electron back-scattering diffraction (EBSD) technique to track the microstructure evolution of the same selected area during interrupted reverse (tension-compression) loading of a Fe-24Mn-3Al-2Si-1Ni-0.06C (wt.%) TWIP steel. Consequently, we report the first direct evidence of de-twinning during load reversal in TWIP steel, in particular, and low SFE polycrystalline fcc materials, in general.

2. EXPERIMENTAL PROCEDURE

The as-cast slab was homogenised at 1100 °C for 2 h, hot rolled to 52% thickness reduction at the same temperature then cold rolled to 42% thickness reduction. A dog-bone shaped tension-compression sample of 4 mm gage length, 4 mm width and 4 mm thickness (these dimensions were chosen to avoid buckling during compression) was wire-cut from the middle of the cold rolled strip such that the gauge

* Corresponding author. E-mail: asaleh@uow.edu.au, telephone: +61 2 4221 3034.

length and width were parallel to the rolling and normal directions, respectively. In order to obtain a fully recrystallized microstructure, the dog-bone sample was annealed at 850 °C, which included 240 s of heating to a stable temperature and 300 s of soaking time followed by immediate water quenching. Thereafter, the tensile sample was mechanically polished up to colloidal silica stage. Uniaxial tension-compression testing was undertaken on a servo-hydraulic universal tester operating in speed control mode at 0.005 mm/s. The test was interrupted at true strains of 12.8% in tension followed by reverse loading in compression back to a true strain of 3.1%.

EBSD was conducted on a JEOL–JSM7001F field emission gun - scanning electron microscope fitted with a Nordlys-II(S) camera and the Oxford Instruments AZtec software suite; operating at 15 kV, ~3 nA and 15 mm working distance. EBSD mapping was conducted on a defined area of interest in the middle of the gage length at true strains of 0 (initial), 12.8% (after forward tension loading, T) and 3.1% (after reverse compression loading, TC), using a constant step size of 0.1 μm.

Post-processing of the EBSD maps was carried out using the Oxford Instruments Channel-5 software package. In all maps, (sub)grain structures are defined by a minimum of three pixels. Low-angle grain boundaries (LAGBs) and high-angle boundaries (HAGBs) comprise misorientations between $2^\circ \leq \theta < 15^\circ$ and $15^\circ \leq \theta \leq 57.5^\circ$ respectively. The twin boundaries (TBs) consist of first order ($\Sigma 3 = 60^\circ \langle 111 \rangle$) and second order ($\Sigma 9 = 38.9^\circ \langle 110 \rangle$) TBs. The maximum deviation of the misorientation angle ($\Delta\theta$) from the exact axis-angle relationship was defined using the Palumbo-Aust criterion (i.e., $\Delta\theta \leq 15^\circ \Sigma^{-5/6}$) [6], resulting in tolerance limits of 6° for $\Sigma 3$ and 2.4° for $\Sigma 9$.

3. RESULTS AND DISCUSSION

Fig. 1 shows the true stress versus strain curve during forward tension loading (T) up to a true strain of 12.8% followed by reverse compression loading (TC) back to a true strain of 3.1%. The corresponding microstructure evolution of the mapped area is presented in Fig. 2 via inverse pole figure maps. The initial recrystallized microstructure (Fig. 2a) comprises equiaxed grains with an average grain size $5.8 \pm 4.5 \mu\text{m}$ (without considering twin boundaries) and a high fraction of annealing twin boundaries.

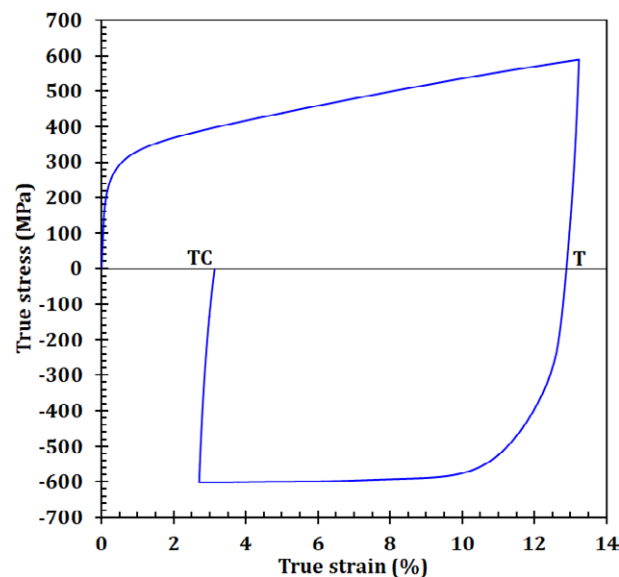


Figure 1. The true stress vs. true strain curve during forward tension (T) – reverse compression (TC) loading.

Forward tension loading (T) to 12.8% true strain led to the instigation of deformation twinning in the form of single lines or parallel packets evolving preferentially in grains with orientations close to $\langle 111 \rangle$ and $\langle 110 \rangle$ parallel to the loading axis (as indicated by the black ovals in Fig. 2b). These deformation twins initiate mostly at the grain and annealing twin boundaries, and in fewer instances they start and finish within a grain. Some in-grain striations were also observed in Fig. 2b, which were ascribed in previous studies to the thickness of individual deformation twins being of the order of tens of nanometres such that they cannot be crystallographically detected via EBSD due to spatial resolution limitations [2, 3]. As the twinning activity increases and the twins stack into relatively thick bundles,

they become eventually detectable by EBSD. Alternatively, rather than interpreting these striations as thin, unindexed twins, other studies have suggested that some of these in-grain striations could be stacking faults that form preferentially at the grain and twin boundaries [7].

Reverse compression loading (TC) back to a true strain of 3.1% resulted in the removal of all deformation twins (as illustrated by the black ovals in Figs. 2(b) and 2(c)). To the best of our knowledge, the former observation provides the first unambiguous evidence of de-twinning during load reversal in TWIP steel, in particular, and low SFE polycrystalline fcc materials, in general.

It is well known that deformation twins in hexagonal close packed (hcp) materials [8-11] can undergo de-twinning (disappearance of the twinned region) upon load reversal via the reverse glide of the partials bounding the twin. This effect is ascribed to the confined number of slip planes in hcp materials, which in turn, sustains the activity on the forward activated twinning systems (allowing for reverse partials glide), rather than activating new slip or twinning systems when reversing the loading direction.

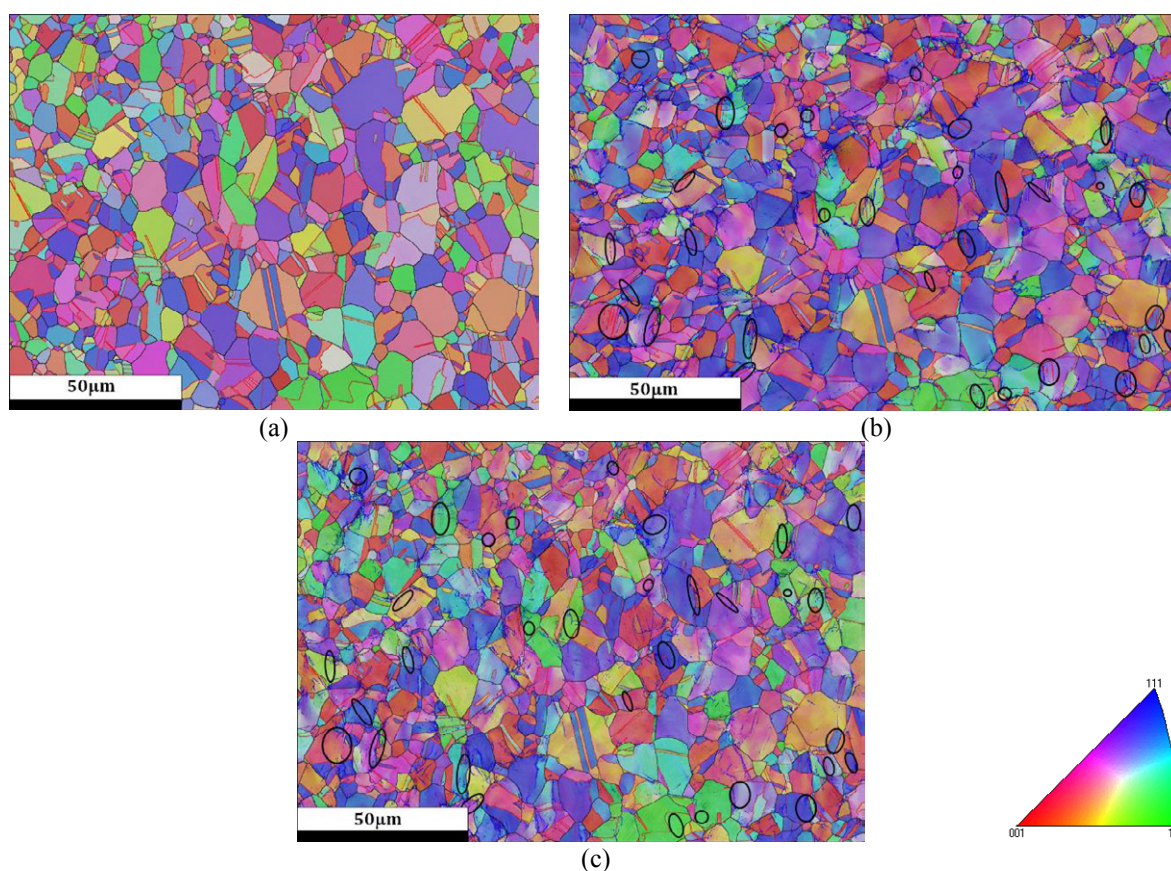


Figure 2. Inverse pole figure maps at true strains of (a) 0, initial, (b) 12.8%, after forward tension loading (T) and (c) 3.1%, after reverse compression loading (TC). LAGBs = blue, HAGB = black, $\Sigma 3$ ($60^\circ\langle 111 \rangle$) = red and $\Sigma 9$ ($38.9^\circ\langle 110 \rangle$) = green. The black ellipses indicate regions where twinning and de-twinning were observed. The loading direction is horizontal.

With regard to fcc materials, de-twinning was observed in Cu-8.5Al single crystals [12] when subjected to compression after the formation of deformation twins during pre-loading in tension. Therein, transmission electron microscopy was used to show that the partial dislocations bounding a deformation twin glide back and forth during loading and unloading. At a certain local critical stress and as these partials glide in the reverse direction, the configuration of the twinned region changes to match the parent grain and the deformation twin disappears. Analogous to the confined slip effect in hcp materials, the former de-twinning mechanism in Cu-8.5Al fcc single crystals is ascribed to the restriction imposed by the existing deformation twins on the number of operative slip planes. Consequently, during reverse loading, the partial dislocations bounding the deformation twin glide in the reverse direction, rather than activating another twin system, and result in de-twinning.

In one of the only studies discussing the possibility of de-twinning in coarse grained polycrystalline

fcc materials, Doquet [13] detected fragmented twins after reverse torsion of low SFE Co-33Ni alloy and suggested that the observed twin fragmentation upon load reversal was due to the interaction between dislocations and twins along the twin-matrix interface which does not allow for the homogenous de-twinning of the entire twin.

In accordance with the above single crystal experiments [12], phase field model simulations of deformation twinning during loading and unloading of a polycrystalline fcc material showed that the partials bounding a deformation twin could glide in the reverse direction upon unloading, and results in de-twinning as the twins are reoriented to match the parent grain [14]. These phase field simulations, therefore, verified the possibility of the reverse glide of the partial dislocations bounding the deformation twin in polycrystalline materials. Lastly, it is highlighted that the reverse glide of the partial dislocations and the associated de-twinning process likely contribute to the pronounced Bauschinger effect (or early yielding during unloading) typically observed during reverse loading of TWIP steels [4, 5].

4. CONCLUSIONS

EBSD mapping of the same selected area provided the first direct experimental evidence of de-twinning during interrupted reverse (tension-compression) loading of TWIP steel, in particular, and low SFE coarse grained polycrystalline fcc materials, in general. This de-twinning process upon load reversal can be attributed to the possibility of the reverse glide of the partial dislocations bounding the deformation twin, which in turn leads to the reorientation of the twin to match the parent grain.

Acknowledgements: This work was financially supported by the Australian Research Council – Discovery Project grant (DP130101882). The JEOL JSM-7001F FEG-SEM was funded by the Australian Research Council – Linkage Infrastructure, Equipment and Facilities grant (LE0882613). The authors are grateful to Prof. D. B. Santos of the Federal University of Minas Gerais, Brazil for providing the as-cast steel.

REFERENCES

- [1] O. Grassel, L. Kruger, G. Frommeyer, L.W. Meyer: *International journal of plasticity* 16 (2000), 1391–1409.
- [2] D. Barbier, N. Grey, S. Allain, N. Bozzolo, M. Humbert, *Materials Science and Engineering: A* 500 (2009), 196–206.
- [3] A.A. Saleh, E.V. Pereloma, A.A. Gazder: *Acta Materialia* 61 (2013), 2671–2691.
- [4] A.A. Saleh, B. Clausen, D.W. Brown, E.V. Pereloma, C.H.J. Davies, C.N. Tomé, A.A. Gazder: *Materials Letters* 182 (2016), 294–297.
- [5] A.A. Saleh, E.V. Pereloma, B. Clausen, D.W. Brown, C.N. Tomé, A.A. Gazder: *Acta Materialia* 61 (2013), 5247–5262.
- [6] G. Palumbo, K. Aust: *Acta Metallurgica et Materialia* 38 (1990), 2343–2352.
- [7] A.A. Gazder, A.A. Saleh, A.G. Kostyryzhev, E.V. Pereloma: *Materials Today: Proceedings* 2 (2015), S647–S650.
- [8] G. Proust, G.C. Kaschner, I.J. Beyerlein, B. Clausen, D.W. Brown, R.J. McCabe, C.N. Tomé: *Experimental Mechanics* 50 (2010), 125–133.
- [9] H. Wang, P.D. Wu, C.N. Tomé, J. Wang: *Materials Science and Engineering: A* 555 (2012), 93–98.
- [10] L. Wu, S.R. Agnew, D.W. Brown, G.M. Stoica, B. Clausen, A. Jain, D.E. Fielden, P.K. Liaw: *Acta Materialia* 56 (2008), 3699–3707.
- [11] H. Wang, P.D. Wu, J. Wang, C.N. Tomé: *International journal of plasticity* 49 (2013), 36–52.
- [12] M.S. Szczerba, S. Kopacz, M.J. Szczerba: *Acta Materialia* 60 (2012), 6413–6420.
- [13] V. Doquet: *Acta Metallurgica et Materialia* 41 (1993), 2451–2459.
- [14] S. Hu, C.H. Jr, L. Chen: *Acta Materialia* (2010), 6554–6564.